S46-34

6 P

OSCILLATORY THERMOCAPILLARY CONVECTION

Jieyong Xu and Abdelfattah Zebib
Department of Mechanical and Aerospace Engineering
Rutgers University
Piscataway, NJ08855-0909

ABSTRACT

Stability analysis of thermocapillary convection in rectangular cavities is performed using direct numerical simulations. Influence of the Reynolds number(Re), the fluid Prandtl number(Pr) and cavity aspect ratio(Ar) on the motion is investigated. Neutral stability curves for transition to time-dependent convection are delineated in the Re - Ar plane for fluids with Pr=1.0, 4.4, 6.78 and 10. Several interesting features of these diagrams are discussed. One important conclusion is that Ar_{cr} increases as Pr decreases. Thus, large values of both Ar and Re are necessary to induce thermocapillary oscillations for small Pr fluids such as liquid metals and semiconductor melts. Energy analysis is also performed for the oscillatory flow in the neighborhood of critical points in order to gain insight into the mechanisms leading to instability.

INTRODUCTION

Understanding fluid motion is crucial in some material processing technologies. In crystal growth from the melt, single crystals with uniform material properties are desired, but homogeneity in crystals can be destroyed if melt motion is unsteady [1]. In the terrestrial environment, buoyancy and thermocapillarity are two major causes for convection. However, in low gravity environment, thermocapillary convection becomes dominant[2].

Numerous experiments (for example, [3], [4] and [5]) have demonstrated the existence of instability of thermocapillary convection, i.e. when the Marangoni number(Ma) exceeds a critical value, the motion undergoes a transition from steady to oscillatory.

Thermocapillary flows have received considerable interest. A rich body of numerical investigations are available in the literature (see [6], [7] and [8]). Results of direct numerical simulation of oscillatory thermocapillary convection was reported in [9] by Peltier & Biringen. They provided a stability diagram in the (Ar, Ma) space for a Pr=6.78 fluid, and found a minimum critical Ar near 2.3 and a minimum critical Ma near 20,000 within the parameter range of Ar$\leq$3.8.

Discussions of instability mechanisms can be found in [10] and [11] for dynamic thermocapillary infinite liquid layers, and in [12] for thermocapillary liquid bridges. Description of the oscillatory instability is also provided in [9], relating the temporal evolution of large-scale structures in the flow and their interaction with the temperature sensitive free surface.

Here, we present a detailed stability diagram for fluids with Pr=10.0, 6.78, 4.4 and 1.0. Interesting features in the diagram are discussed. Comparison of flow patterns is provided to investigate the influence of Re and Ar on the motion of a Pr=10 fluid. In addition, energy analysis results are also given for convection of a Pr=4.4 fluid with Re near both higher and lower critical points of the unstable region at Ar=3.0.

MODEL DESCRIPTION AND NUMERICAL PROCEDURE

The physical model considered is thermocapillary convection of incompressible and Newtonian fluid in a rectangular cavity with height H and width Ar x H (Ar is the aspect ratio). Two vertical isothermal side walls are kept at T_h on the left and T_c on the right, respectively. Bottom boundary is rigid and adiabatic. Top boundary is a flat free surface open to a passive gas. Here, surface tension on the free surface is assumed to be a linear function of temperature as $\sigma = \sigma_0 - \gamma(T - T_0)$.

A dimensionless mathematical model in the stream function - vorticity formulation is used for numerical simulation, in which length, temperature, velocity and time are made dimensionless by use of scales H, $\Delta T = (T_h - T_c)$, $\gamma \Delta T/\mu$ and H^2/ν, respectively. Dimensionless parameters are defined as: $\mathrm{Pr} = \frac{\nu}{\alpha}$ and $\mathrm{Re} = \gamma \frac{\Delta T H}{\mu \nu}$, where μ, ν and α are dynamic viscosity, kinematic viscosity and thermal diffusivity, respectively.

The coupled equation system is solved by a finite volume based scheme, in which the Poisson equation for the stream function is solved by the SOR method. Both the vorticity transport and energy equations are solved by the alternating direction implicit(ADI) method. All time derivatives and spatial derivatives including boundary conditions are approximated in second order accuracy. Velocities are obtained as spatial derivatives of stream function. Uniform mesh is used in the solution procedure with mesh resolution of 50 to 90 points per dimensionless unit length, depending on the Reynolds number considered.

RESULTS

For thermocapillary convection of a Pr=6.78 fluid in rectangular cavities, Peltier & Biringen [9] constructed a stability diagram in the (Ar, Ma) plane for the region Ar $\leq$3.8 and Ma$\leq$1.0x10^5. Their Ma is equivalent to our RePrAr. Some interesting characteristics were found, including the existence of double valued stability limits, i.e. as Ma goes up, the flow first changes from stable to oscillating at Ma_{cr1}, and then becomes stable again when Ma_{cr2} is reached. Ma_{cr2} grows monotonically with Ar, however, Ma_{cr1} does not.

In the present work, we extend this investigation to fluids with Pr=1.0, 4.4 and 10.0, and construct the stability diagrams in the (Ar, Re) plane. A wider range of parameter space ($0.0 \leq$ Ar ≤ 7.0 and $0.0 \leq$ Re $\leq 1.3\mathrm{x}10^4$) is considered as shown by Fig. 1, in which more interesting features are found. If we look at the particular fluid with Pr=4.4, the first critical aspect ratio is around 2.6. Unstable region exists for any Ar>2.6, and more interestingly, there are more than one unstable regions with Ar>6.0, i.e. if Re goes up from zero, one can find that the flow is steady at low Re, starts to oscillate at first critical point, goes back to steady state at second critical point, and becomes oscillatory again as Re reaches its third critical point. In addition, stability curves of fluids with different Pr do not cross each other. Neutral curves of smaller Pr fluids always locate inside curves of larger Pr, i.e. when Pr goes smaller, the critical aspect ratio always becomes larger, so does the lowest critical Reynolds number. From the trend given by these curves, we can draw a very important conclusion that, for fluids with very low Pr, large values of critical Ar and Re are expected for the transition to oscillatory thermocapillary convection.

The convective flow field is strongly influenced by Re, Ar and Pr. For a Pr=10 fluid, Fig. 2 gives three examples of streamlines at Ar=3.0 and Ar=6.0. (a) shows the flow field at Re_{cr1} for Ar=3.0, in which one can see a bi-cellular structure with a stronger cell near the hot wall and a much weaker cell close to the cold wall. Increasing Re to Re_{cr2} at about 7400, one can find, in (b), that the previous strong hot wall cell moves to the center of the cavity, and the weak cell disappears. For a larger aspect ration (Ar=6.0), Fig. 2 (c) exhibits the flow pattern at Re_{cr1}, from which we find that three cells exist, with the strongest one still near the hot wall. Further increase of Ar will result in more cellular structure in the flow field.

For convection of a Pr=10 fluid at a large aspect ratio (Ar=20), Fig. 3 displays the mean velocity profiles and snapshots of temperature fluctuation fields for three different values of Re=1012, 1025 and 1500, respectively. Comparison of these three mean velocity profiles shows almost identical patterns even when Re changes from 1012 to 1500, with most strong activities locating near two side walls. However, large difference can be found among the temperature fluctuation fields. At Re=1012 (b-1), which is very close to Re_{cr1}, a *thermal wave* generates near the center of the cavity and starts to die at the right edge of the strong flow cell near the hot wall. Most area in the right part of the cavity remains pretty calm. The *wave* actually propagates toward the hot wall if we look at snapshots at different time instants, which is in agreement with [10]. As Re goes up a little bit to 1025, (b-2) shows that the starting point of the *thermal wave* moves toward the cold wall. Further increase Re, this starting point keeps moving to the right until it reaches the cold wall. Fig. (b-3) shows the case when Re=1500, in which one can see a *wave* generating at the cold wall, propagating actively, and dying at the right edge of the strong flow cell near the hot wall.

ENERGY ANALYSIS

Energy analyses are performed for flows with Reynolds numbers in the neighborhoods of different critical points. The physical parameters of the oscillatory flows are decomposed into their mean and fluctuating components, and investigations are conducted on the behavior of the fluctuation kinetic energy (k) and the fluctuation thermal energy($\theta = t^2/2$).

For the case Ar=3.0 and Pr=4.4, results of the energy analysis are provided here for flows with Reynolds numbers near both lower(Re=1950) and higher(Re=5020) critical points of the unstable region. Temporal variations over one flow oscillation period are shown in Fig. 4(a-1) and (a-2) for the rate of change of the total fluctuation kinetic energy($dK/d\tau = \frac{d}{d\tau}(\int k d\Omega)$, as well as its components I_{k_1}(production), I_{k_2}(diffusion) and I_{k_3}(dissipation). It is seen that $dK/d\tau$ oscillates with its time average being equal to zero, which means no kinetic energy is added to the flow over each period of oscillation. This is consistent with the fact that the flow field oscillates with a stable amplitude. If we look at I_{k_1}, I_{k_2} and I_{k_3}, we find I_{k_1} and I_{k_3} providing two major contributions, with I_{k_1} always being positive (destabilizing) and I_{k_3} always being negative (stabilizing). Time averages of I_{k_1} and I_{k_3} are much larger than that of I_{k_2}, however, the phase difference between I_{k_1} and I_{k_3} is always near π, which means that I_{k_3} always cancels the effect of I_{k_1}. This gives the smaller term I_{k_2} a chance to influence the temporal behavior of $dK/d\tau$. In Fig. 4(a-2), which is for the higher critical point, one can clearly see that $dK/d\tau$ oscillates at a very close amplitude and a very small phase difference with I_{k_2}, while the phase difference between I_{k_1} and I_{k_3} is almost π.

Variation of the rate of change of the total fluctuation thermal energy ($d\Theta/d\tau = \frac{d}{d\tau}(\int \theta d\Omega)$ and its components (I_{t_1} and I_{t_2}) are given in Fig. 4(b-1) and (b-2) for the lower and higher critical points, respectively. As expected, $d\Theta/d\tau$ oscillates with its time average being equal to zero, since the temperature field oscillates in a limit cycle with stable amplitude. In addition, although the time averages of I_{t_1} and I_{t_2} have the same absolute value, the oscillation amplitude of I_{t_1} is much larger than that of I_{t_2}. Thus I_{t_1} dominates the oscillatory behavior of $d\Theta/d\tau$. In both cases, the phase difference between I_{t_1} and $d\Theta/d\tau$ is very small. If we further compare the magnitude of the destabilizing fluctuation thermal energy component (I_{t_1}) and the kinetic energy components (I_{k_1} and I_{k_2}), we find that the magnitude of thermal energy production I_{t_1} is generally two to three orders larger than that of I_{k_1} or I_{k_2}. Thus, I_{t_1} appears to be the major driving source of flow instability.

CONCLUSIONS

Direct numerical simulation is employed for stability analyses of thermocapillary driven convection in rectangular cavities. Stability boundaries are delineated in the Re - Ar plane, in which several interesting features are found. Influence of Re and Ar on the flow patterns and the temperature fields is briefly discussed. In addition, energy analyses are performed to gain insight into mechanisms involved in the onset of instability. Results are presented for a Pr=4.4 fluid with Re near both higher and lower critical points at Ar=3.0. Investigations on 2D and 3D convection of lower Pr as well as larger Ar and Re are in progress.

ACKNOWLEDGEMENT

This research is sponsored by NASA through grant No. NAG3-1453. We also acknowledge the Pittsburgh Supercomputing Center for providing CRAY C90 time through grant No. CTS950032P.

References

[1] Hurle, D. T. J. *Thermo-hydrodynamic oscillation in liquid metals: the cause of impurities striations in melt-grown crystals.* J. Phys. Chem. Solids, Suppl. no.1, 659-669(1967).

[2] Ostrach, S. *Low-gravity fluid flows.* Ann. Rev. Fluid Mech., **14**, 313-345(1982).

[3] Chun, C. H. and Wuest, W. *Experiments on the transition from the steady to the oscillatory Marangoni convection of a floating zone under reduced gravity effect.* Acta Astronautica, **6**, 1073-1082(1979).

[4] Chun, C. H. *Experiments on the transition from the steady to the oscillatory temperature distribution in a floating zone due to Marangoni convection.* Acta Astronautica, **7**, 479-488(1980).

[5] Preisser, F., Schwabe, D., and Scharmann, A. *Steady and oscillatory thermocapillary convection in liquid columns with free cylindrical surface.* J. Fluid Mech., **126**, 545-567(1983).

[6] Zebib, A., Homsy, G. M. and Meiburg, E. *High Marangoni number convection in a square cavity.* Physics Fluids, **28**(12), 3467-3476(May 1985).

[7] Carpenter, Bradley M. and Homsy, G. M. *High Maragoni number convection in a square cavity: Part II.* Physics Fluids A, **2**(2), 137-149(1990).

[8] Ben Hadid, H. and Roux, B. *Thermocapillary convection in long horizontal layers of low-Prandtl number melts subject to horizontal temperature gradient.* J. Fluid Mech., **221**, 77-103(1990).

[9] Peltier, L. J. and Biringen S. *Time-dependent thermocapillary convection in a rectangular cavity: numerical results for a moderate Prandtl number fluid.* J. Fluid Mech., **257**, 339-357(1993).

[10] Smith, Marc K. and Davis, Stephen H. *Instabilities of dynamic thermocapillary liquid layers. Part 1. Convective instabilities.* Physics Fluids, **132**, 119-144(1983).

[11] Smith, Marc K. *Instability mechanisms in dynamic thermocapillary liquid layers.* Physics Fluids, **29**(10), 3182-3186(1986).

[12] Wanschura, M., Shevtsova, V. M., Kuhlmann, H. C. and Rath, H. J. *Convective instability mechanisms in thermocapillary liquid bridges.* Physics Fluids, **7**(5), 912-925(May 1995).

[13] Braunsfurth, M. G. and Homsy, G. M. *Experimental study of buoyant-thermocapillary convection in a rectangular cavity.* 48th annual meeting of APS-DFD, (presentation FG3), (1995).

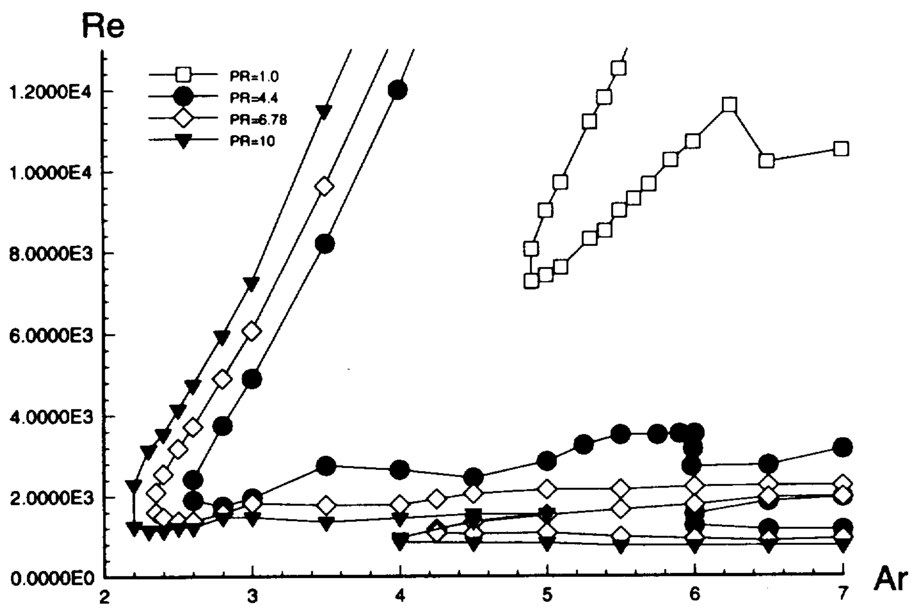

Figure 1: Stability diagrams in the Re - Ar plane for fluids with Pr=10.0, 6.78, 4.4 and 1.0.

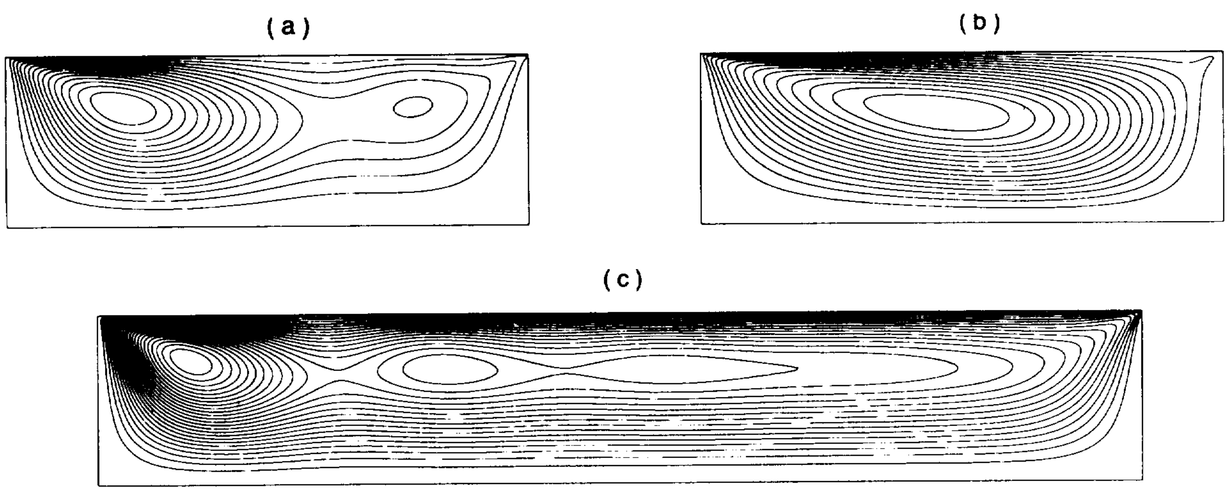

Figure 2: Examples of streamlines for convection of a Pr=10 fluid. Case (a): Ar=3.0, Re=1530 ($\approx$ the first critical number); Case (b): Ar=3.0, Re=7400 ($\approx$ the second critical number); Case (c): Ar=6.0, Re=700 ($\approx$ the first critical number).

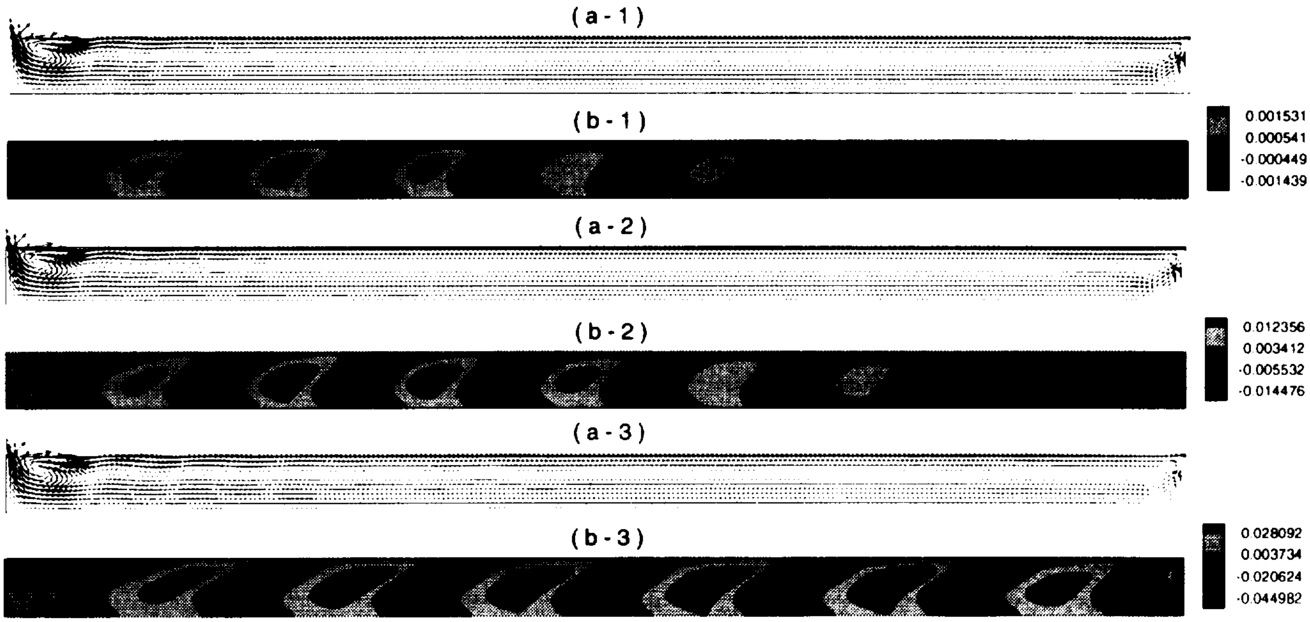

Figure 3: Comparison of mean velocity profiles and temperature fluctuation fields of a Pr=10 fluid at large aspect ratio Ar=20. Case 1: Re=1012, which is approximately the first critical point; Case 2: Re=1025, which is slightly higher than the first critical point; Case 3: Re=1500, which is much higher than the first critical point.

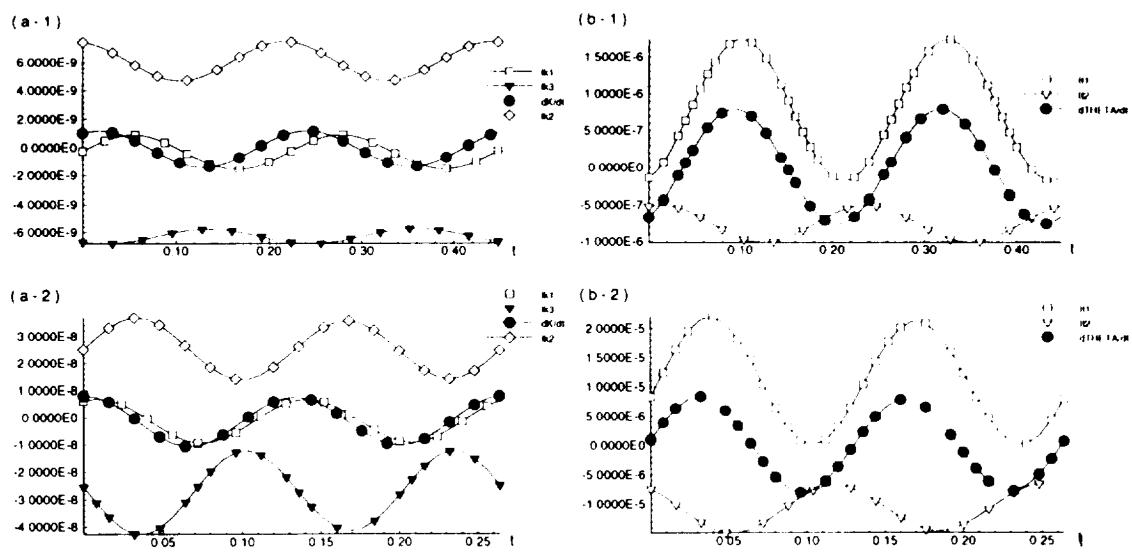

Figure 4: Temporal variation of the rate of change of the total kinetic energy $\frac{dK}{d\tau}$, the thermal energy $\frac{d\Theta}{d\tau}$ and their components I_{k_1}, I_{k_2}, I_{k_3}, I_{t_1} and I_{t_2} for a Pr=4.4 fluid at Ar=3.0. (a-1) and (b-1) give results for Re=1950 (near the lower critical point), (a-2) and (b-2) provide results for Re=5020 (near the higher critical point).